RESEARCH ARTICLE | *Neural Development of the GI Tract*

Development of the intrinsic innervation of the small bowel mucosa and villi

 Marlene M. Hao,[1,2] Candice Fung,[1] Werend Boesmans,[1,3,4] Katrien Lowette,[1] Jan Tack,[1] and Pieter Vanden Berghe[1]

[1]*Laboratory for Enteric Neuroscience, Translational Research Center for Gastrointestinal Disorders, University of Leuven, Belgium;* [2]*Department of Anatomy and Neuroscience, the University of Melbourne, Australia;* [3]*Department of Pathology, GROW, School for Oncology and Developmental Biology, Maastricht University Medical Center, The Netherlands; and* [4]*Biomedical Research Institute, Hasselt University, Hasselt, Belgium*

Hao MM, Fung C, Boesmans W, Lowette K, Tack J, Vanden Berghe P. Development of the intrinsic innervation of the small bowel mucosa and villi. *Am J Physiol Gastrointest Liver Physiol* 318: G53–G65, 2020. First published November 4, 2019; doi:10.1152/ajpgi.00264.2019.—Detection of nutritional and noxious food components in the gut is a crucial component of gastrointestinal function. Contents in the gut lumen interact with enteroendocrine cells dispersed throughout the gut epithelium. Enteroendocrine cells release many different hormones, neuropeptides, and neurotransmitters that communicate either directly or indirectly with the central nervous system and the enteric nervous system, a network of neurons and glia located within the gut wall. Several populations of enteric neurons extend processes that innervate the gastrointestinal lamina propria; however, how these processes develop and begin to transmit information from the mucosa is not fully understood. In this study, we found that Tuj1-immunoreactive neurites begin to project out of the myenteric plexus at embryonic day (E)13.5 in the mouse small intestine, even before the formation of villi. Using live calcium imaging, we discovered that neurites were capable of transmitting electrical information from stimulated villi to the plexus by E15.5. In unpeeled gut preparations where all layers were left intact, we also mimicked the basolateral release of 5-HT from enteroendocrine cells, which triggered responses in myenteric cell bodies at postnatal day (P)0. Altogether, our results show that enteric neurons extend neurites out of the myenteric plexus early during mouse enteric nervous system development, innervating the gastrointestinal mucosa, even before villus formation in mice of either sex. Neurites are already able to conduct electrical information at E15.5, and responses to 5-HT develop postnatally.

NEW & NOTEWORTHY How enteric neurons project into the gut mucosa and begin to communicate with the epithelium during development is not known. Our study shows that enteric neurites project into the lamina propria as early as E13.5 in the mouse, before development of the submucous plexus and before formation of intestinal villi. These neurites are capable of transmitting electrical signals back to their cell bodies by E15.5 and respond to serotonin applied to neurite terminals by birth.

enteric nervous system development; gut mucosa; neurite extension; serotonin

Address for reprint requests and other correspondence: P. Vanden Berghe, KU Leuven, TARGID, Herestraat 49, O&N1, Box 701, 3000 Leuven, Belgium (e-mail: pieter.vandenberghe@kuleuven.be).

INTRODUCTION

The lumen of the gastrointestinal tract is a complex milieu of ingested nutrients, waste products, and microbiota that are separated from the body by a layer of intestinal epithelial cells. Receiving and interpreting information about luminal contents is important not only for gastrointestinal function, but also has an impact on many other body systems, including control of food intake and host defense (20). The enteric nervous system (ENS) is a network of neurons and glia located within the wall of the gastrointestinal tract that is vital for control of gut function and plays a crucial role in detecting gut contents. Intrinsic primary afferent neurons (IPANs), also known as intrinsic sensory neurons with Dogiel type II morphology and afterhyperpolarizing (AH) electrophysiological characteristics (19), have cell bodies that are located within the plexus layers of the gut and extend processes toward the gut mucosa. Although these IPANs are present in both the myenteric and submucous plexus in guinea pig (34, 35), they have not been conclusively identified in the submucous plexus of mice (40, 52). Secretomotor and vasodilator neurons also project into the mucosa. In mice and other small mammals, these neurons generally have cell bodies in the submucous plexus and control fluid secretion (18).

Information from the gut lumen is relayed to the nervous system via enteroendocrine cells, which are dispersed among the epithelial cells that line the gut mucosa surface (23). Many elegant studies have shown that in response to chemical and mechanical stimuli, serotonin (5-hydroxytryptamine, 5-HT) is released from one type of enteroendocrine cell, the enterochromaffin cells (1, 3, 5, 12, 34, 35, 38). It has been assumed that this 5-HT then acts on the processes of IPANs in the enteric nervous system; however, this has not been definitively proven. Studies from several laboratories have now shown that 5-HT released from the gut mucosa is not necessary for establishing gut motility (2, 32, 51, 53, 59), but it does have a role in modulating colonic propulsions (26, 47). Whether, and to what extent, enteric neurons respond to 5-HT in the mucosa and how this could then have an impact on other aspects of gut function has not yet been examined. Interestingly, enteroendocrine cells have recently been found to synapse with vagal neurons and directly communicate information from the gut lumen to the brain (31).

Communication between enteroendocrine cells and the ENS is important after birth, but little is known about the development of this communication. In the developing mouse, motility

of the duodenum is under neural control by embryonic day (E)18.5, just before birth (45). Neurons with AH type electrophysiology and Dogiel type II morphology have been identified in the postnatal gut (17); however, it is not known how and when intrinsic sensory neurons develop their stereotypical mucosal projections and begin to receive information from the gut lumen. Previously, neurites have been identified in the mucosa of the mouse small intestine at E16.5 (10) and E18.5 (57). However, in a recent study, neurites were reported to be absent in the villi of wild-type mice at E18.5, but were present in mutant mice that had defects in the hedgehog signaling pathway (29).

In our current study, we identified enteric neurites extending from the myenteric plexus layer of the small intestine at E13.5 and innervating the basolateral surface of the epithelial cell layer by E14.5. Using calcium imaging and electrical stimulation, we showed that neurites are capable of transmitting electrical information back to the plexus by E15.5. In addition, we showed that enteric neurons are capable of responding to 5-HT applied to the gut mucosa, and that this starts at postnatal day (P)0, with considerable postnatal maturation.

METHODS

Ethical approval and mice strains. Wnt1-Cre;R26R-GCaMP3 mice were generated by mating *Wnt1-Cre* [Research Resource Identifiers (RRID): MGI:2386570] (15) with *R26R-GCaMP3* mice (RRID: IMSR_JAX:014538; from The Jackson Laboratory, Bar Harbor, ME) (60). All neural crest-derived cells in these embryos express the genetically encoded calcium indicator GCaMP3 (8). Wild-type C57BL6 mice and *ChAT-Cre;R26R-YFP* mice were also used for immunohistochemical studies. *ChAT-Cre;R26R-YFP* mice were generated by mating *ChAT-Cre* mice (RRID: IMSR_JAX:031661) with floxed YFP mice (RRID: IMSR_JAX: 006148). Midday of the day on which a plug was found was designated E0.5. All mice were housed in rooms with standard light-dark cycles and fed ad libitum with standard chow. Adult mice were killed by cervical dislocation or CO_2 asphyxiation followed by cervical dislocation, and embryos were decapitated immediately upon removal. Mice of both sexes were used in experiments, and no discrimination was made between male or female at any embryonic or postnatal ages. Experiments were performed in accordance with the ethical guidelines of the University of Leuven (KU Leuven) and the University of Melbourne. All experiments were approved by the Anatomy & Neuroscience, Pathology, Pharmacology and Physiology Animal Ethics Committee of the University of Melbourne (project no. 1112330) and the Animal Ethics Committees of KU Leuven (project no. 192/2013).

Tissue preparation and immunohistochemistry. Small intestine from E13.5, E14.5, E15.5, E16.5, P0, and adult (~3 mo old) wild-type C57BL6, *Wnt1-Cre;R26R-GCaMP3*, or *ChAT-Cre;R26R-YFP* mice were dissected in Krebs solution (in mM: 120.9 NaCl, 5.9 KCl, 1.2 $MgCl_2$, 1.2 NaH_2PO_4, 14.4 $NaHCO_3$, 2.5 $CaCl_2$, and 11.5 glucose) and fixed in 4% formaldehyde in phosphate buffered saline (PBS) for 1 h. The rostral half of the small intestine (including the duodenum and rostral jejunum) was used for all embryonic immunohistochemical experiments. For cryosections, the rostral small intestine was washed and placed in PBS containing 30% sucrose as a cryoprotectant, stored overnight at 4°C, then embedded in OCT compound (Tissue-Tek), and frozen in liquid nitrogen. Then 10-μm, 20-μm, and 40-μm-thick frozen sections were cut transversely through the entire thickness (all layers) of the gut and collected on polylysine-coated slides for immunohistochemistry. For whole mount three-dimensional (3D) confocal scans, the small intestine was first opened along the mesenteric border before fixation.

All preparations for immunohistochemistry were blocked for 2 h in PBS containing 0.5% Triton-X and 4% donkey serum and incubated in primary antisera at 4°C overnight (Table 1). All antibodies have been previously tested on postnatal and adult mouse tissue and have been found to label the correct cell populations. After washing in PBS, samples were incubated in secondary antisera for 2 h at room temperature: donkey anti-rabbit Alexa Fluor 488 (1:1,000; Molecular Probes, A21206; RRID:AB_141708); donkey anti-sheep FITC (1:100; Jackson 713-095-003; RRID:AB_2340718); donkey anti-rabbit Alexa Fluor 594 (1:1,000; Molecular Probes A21207, RRID: AB_141637); donkey anti-sheep Alexa Fluor 594 (1:100; Molecular Probes, A11016; RRID:AB_10562537); donkey anti-mouse Alexa Fluor 594 (1:1,000; Molecular Probes, A21203; RRID:AB_141633); donkey anti-sheep Alexa Fluor 647 (1:500; Molecular Probes A21448; RRID:AB_1500712), and DAPI (1:5000; Invitrogen).

All preparations were imaged on a Zeiss LSM780 or LSM880 laser-scanning confocal microscope.

Immunohistochemical analysis. For quantifying neuronal fibers in cryosections, a minimum of five sections were examined for each gut

Table 1. *Primary antisera*

Antibody Name	Dilution	Company, Cat. No.	RRID
Rabbit anti-neuronal class III β-tubulin (Tuj1)	1:2,000	Covance, PRB-435P-100	AB_291637
Mouse anti-Tuj1	1:2,000	Covance, MMS-435P	AB_2313773
Goat anti-GFP	1:400	Rockland, 600–101–215	AB_218182
Rabbit anti-GFP	1:500	Molecular Probes, A11122	AB_221569
Sheep anti-NOS	1:2,000	From Dr. Piers Emson	
Rabbit anti-neurofilament M	1:1,000	Chemicon, AB1987	AB_91201
Goat anti-CGRP	1:1,000	Bio-Rad, 1720–9007	AB_2290729
Mouse anti-HuC/D	1:500	Molecular Probes, A21271	AB_221448
Goat anti-Sox10	1:300	Santa Cruz Biotechnologies, sc17342	AB_2195374
Rabbit anti-calbindin	1:1,600	Swant CB-38a	AB_10000340
Rabbit anti-calbindin	1:1,000	Chemicon AB149	AB_2307441

CGRP, calcitonin gene-related peptide; GFP, green fluorescent protein; NOS, nitric oxide synthase; RRID, Research Resource Identifier.

sample, and a sample was counted as "positive" if immunoreactive fibers were identified in any section. For counting submucous plexus cells, whole transverse cryosections through all gut layers from *Wnt1-Cre;R26R-GCaMP3* mice were imaged, and GCaMP+ cells located in the submucous plexus were counted. GCaMP+ cells were identified using antisera against GFP. Sox10+ or Hu+ cells were then counted and calculated as a proportion of the total number of GCaMP+ cells. Myenteric plexus cells were counted in the same fashion. For post hoc analysis of cells after live calcium imaging, imaged preparations were fixed and processed for immunohistochemistry, as above. The location of cells was identified by noting the relative location of the field of view that was imaged and the shape and orientation of the ganglia. For measurement of Hu+ cells, their diameters were measured at their longest point using ImageJ (National Institutes of Health, Bethesda, MD).

Live calcium imaging. For imaging experiments, the rostral small intestine was dissected from E14.5, E15.5, E16.5, P0, P7, and adult *Wnt1-Cre;R26R-GCaMP3* mice and placed in Krebs solution bubbled with carbogen (5% O_2-95% CO_2) throughout the duration of the experiment. For embryonic gut preparations, the opened gut was suspended on Millipore filter paper with a window cut out to maintain the 3D structure of the villi. For postnatal and adult preparations, dissections were carried out in Sylgard-lined dishes. The gut was opened along the mesenteric border, and the contents were flushed out. The whole gut, including all tissue layers, were then stretched over a stainless-steel inox ring and immobilized by a matched rubber

O-ring, as previously described (50). The inox rings are custom-made, 5–7 mm in diameter, with a 0.5-mm wide lip, and are 2 mm in height. Tissue was firmly stretched over the ring to reduce muscle contractions and movement during recording. Technical drawings of the inox rings can be made available upon request (please contact P. Vanden Berghe: pieter.vandenberghe@kuleuven.be). Preparations were placed in glass coverslip-bottom chambers and imaged with a Zeiss Axiovert 200M microscope equipped with a monochromator (Poly V) and a cooled charge-coupled device camera (Imago QE), both from TILL Photonics. GCaMP3 was excited at 470 nm, and its fluorescence emission collected at 525 nm using a ×20 (NA 0.75) objective. Images were collected using TILLVISION software (TILL Photonics), and analysis was performed using custom-written macros in IGOR PRO (Wavemetrics; available for download via www.targi-d.eu, select LENS).

Regions of interest (ROIs) were drawn over each cell, and fluorescence intensity was calculated and normalized per ROI to its baseline starting value. All recordings were performed at room temperature, and all preparations were constantly perfused with Krebs solution bubbled with carbogen with 1 μM nifedipine to reduce muscle contractions. Changes in fluorescence intensity were calculated and expressed as a fraction of the baseline fluorescence, as F/F_0. Peaks in $[Ca^{2+}]_i$ were individually determined, with a minimum increase of five times the intrinsic noise level. The amplitude of the $[Ca^{2+}]_i$ peak was calculated as the maximum increase in $[Ca^{2+}]_i$ above baseline ($\Delta F/F_0$). In many cases, muscle contractions caused displacement of the
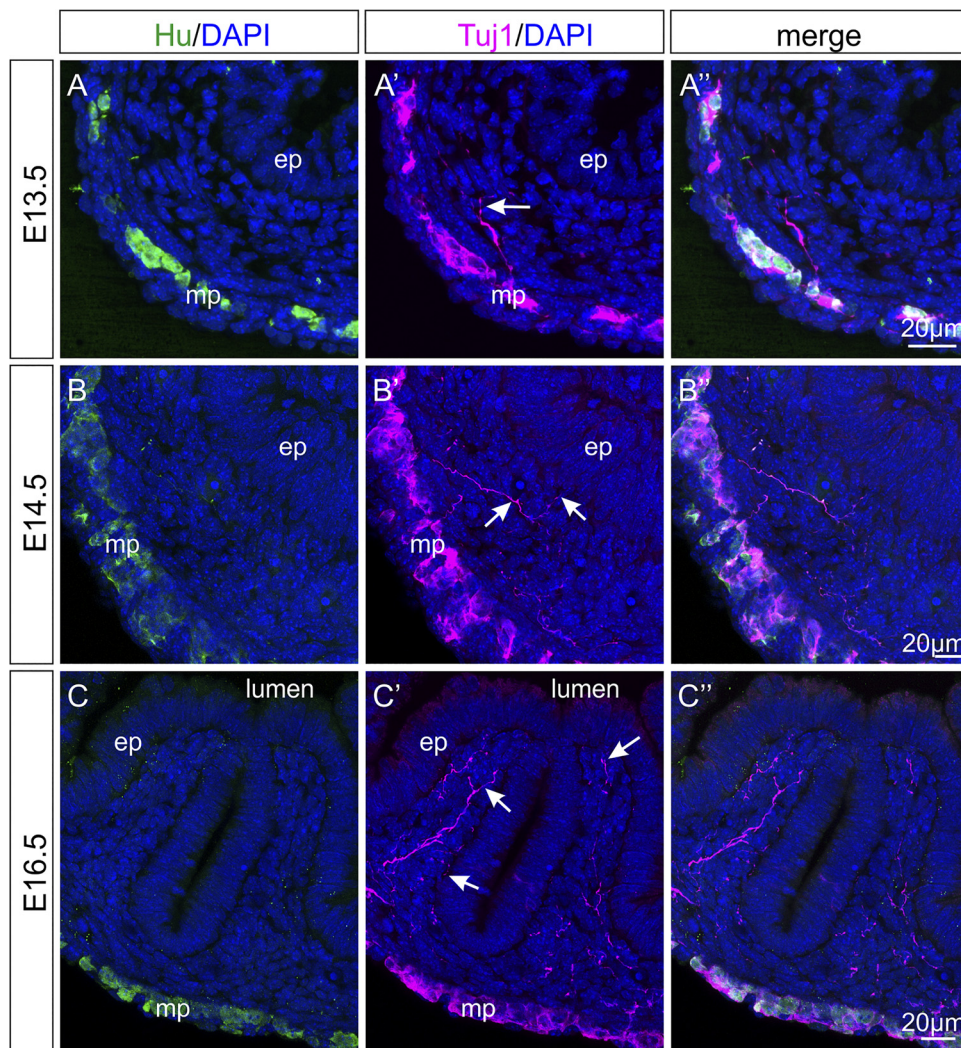

Fig. 1. Neurite projections in embryonic rostral small intestine. Transverse cryosections at E13.5 (*A–A"*), E14.5 (*B–B"*), and E16.5 (*C–C"*) with immunohistochemistry performed against Hu, Tuj1 and DAPI. Tuj1+ fibers extend into the mucosa at E13.5 (arrows), some of which can be seen contacting the basolateral surface of the epithelium by E14.5. Many more Tuj1+ fibers are present at E16.5; however, the majority of Hu-positive cell bodies are located in the myenteric and not submucous plexus. All scale bars = 20 μm.

tissue. Custom written macros were used to reduce displacement in movies post hoc. In the majority of cases, the movement occurred after the maximum $[Ca^{2+}]_i$ peak; therefore, the displacement did not disturb the measurement of $[Ca^{2+}]_i$ transient amplitude.

Electrical stimulation. Electrical stimulation was applied as a train of 300-μs pulses at 20 Hz for 1 s using a focal electrode placed on the tip of a villus (50-μm diameter Tungsten wire), coupled to a Grass stimulation unit (amplitude 30 V). Tetrodotoxin (TTX; 1 μM; Sigma) or hexamethonium (200 μM; Sigma) was diluted in Krebs solution with nifedipine and perfused in the organ bath for a minimum of 10 min before recording. For all drug recordings, ganglia in the same field of view were stimulated twice, the first time in control Krebs solution, and then a second time after 10 min wash-in of the drug.

5-HT spritz application. 5-HT (10 μM, Sigma) was applied by pressure ejection from a micropipette (tip diameter 10–20 μm) using Picospritzer II (10 psi, 2 s, General Valve Corporation). To examine the effect of 5-HT application onto the epithelial surface, the micropipette was placed adjacent to a villus for pressure ejection. To examine responses to 5-HT injected into the mucosa for application directly onto neurite terminals, the micropipette was first placed adjacent to a villus and given a gentle tap to push the tip through the external epithelial cell layer. To calculate the volume of solution injected, the micropipette was placed within an oil droplet, and the volume of aqueous solution ejected was calculated from the diameter of the resulting sphere. Ondansetron (10 μM; Sigma) and hexamethonium (200 μM; Sigma) was diluted in Krebs solution with nifedipine and perfused in the organ bath for a minimum of 10 min before recording.

Again, for each drug, ganglia in the same field of view were stimulated twice, the first time 5-HT was injected while tissue was perfused in control Krebs solution, and the second time, 5-HT was injected after a 10-min wash-in of the drug. Time controls were also performed where the 5-HT was injected twice in control Krebs solution only, 10 min apart.

Experimental design and statistical analysis. All data were collected from different gut preparations (*n*) isolated from different animals (pups from a minimum of two independent litters) for each experimental condition at each embryonic or postnatal age. Experimental design for calcium imaging, electrical stimulation, and 5-HT injections are described above. For the majority of data sets, *n* represents the number of gut preparations examined, unless otherwise stated. All data are shown as means ± SE. To compare calcium responses across different ages, one-way ANOVA was used with a Bonferroni post hoc test. To examine responses in the presence of different drugs, paired Student's *t* tests were used to examine the evoked $[Ca^{2+}]_i$ amplitude for each cell in control conditions and after drug wash-in. Results were considered significant if $P < 0.05$.

RESULTS

Enteric neurites project out to the epithelium at E13.5 one day before villus formation. Villi develop in the mouse small intestine from E14.5 to E15.5 (41). To examine neurite projections to the developing lamina propria, transverse sections of rostral small intestine from E13.5 and E16.5 mice were
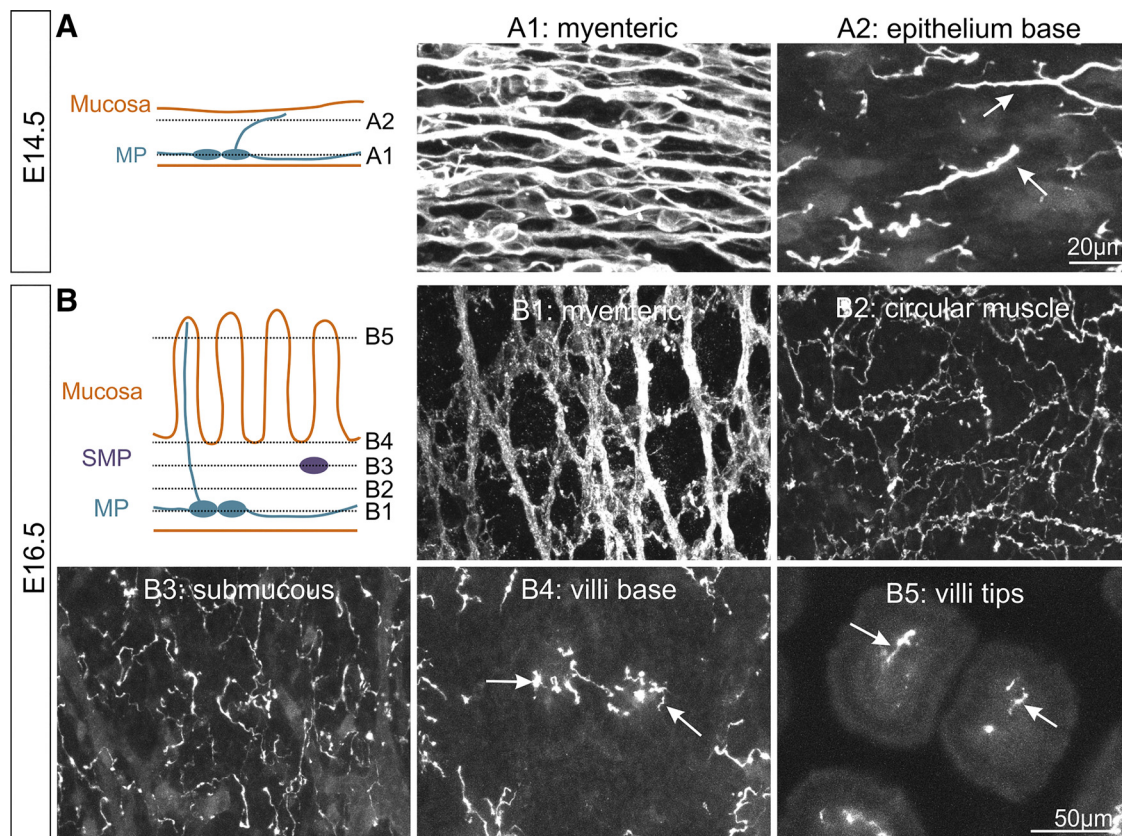

Fig. 2. Confocal imaging of Tuj1-immunoreactive fibers through whole mount preparations of embryonic gut at E14.5 (*A1–A2*) and E16.5 (*B1–B5*). The locations of each scan are shown diagrammatically in *A* and *B*. Many Tuj1+ cell bodies and fiber bundles are present in the myenteric plexus at E14.5 (*A1*), as well as at the base of the epithelium (*A2*). Both *A1* and *A2* were imaged from the same location on the tissue, at different levels through the radial plane. At E16.5, there is greater separation of individual ganglia in the myenteric plexus, interconnected by Tuj1+ fibers (*B1*), which also extend into the circular muscle layer (*B2*). There are few Tuj1+ cell bodies in the submucous plexus, but fibers are still present, presumably from the myenteric plexus (*B3*). Tuj1+ fibers extend from the base of villi (*B4*, arrows) into their tips (*B5*, arrows). Likewise, images *B1–B5* were taken from the same location on the tissue, at different levels through the radial plane.

immunostained with the pan-neurite marker, Tuj1. Tuj1-immunoreactive neurites were observed in the lamina propria in all gut preparations examined at all four ages ($n = 3/3$ for E13.5, $n = 5/5$ for E14.5, $n = 8/8$ for E15.5, and $n = 5/5$ for E16.5). Previous studies in mice have shown that the first neural crest-derived cells settle on the outer side of the circular muscle layer in the location of the myenteric plexus, and submucosal ganglia form several days later from a secondary, centripetal, migration of myenteric cells (28). At E13.5, Tuj1-immunoreactive neurites appeared to project from the presumptive myenteric plexus toward the mucosa (Fig. 1*A*), and some processes extended to the basolateral surface of the epithelial cells by E14.5 (Fig. 1*B*). Villi could be morphologically detected at E15.5 (data not shown) and E16.5, and there were abundant Tuj1+ neurites projecting to the epithelial cell layer at the tips, as well as near the bases of villi (Fig. 1*C*).

Immunohistochemistry was also performed on whole-mount gut preparations with all tissue layers intact. 3D confocal scans through the E14.5 and E16.5 rostral small intestine revealed many Tuj1-immunoreactive fibers in the developing lamina propria at both ages (Fig. 2, Supplemental Movies S1 and S2: http://doi.org/10.5281/zenodo.3518046 and http://doi.org/10.5281/zenodo.3518194, respectively). Though Tuj1-immunoreactive fibers may appear sparse in the 10- to 40-μm-thick cryosections, whole-mount preparations show that Tuj1 fibers are present throughout the lamina propria (compare Figs. 1*C* and 2*B*). At E14.5, there was an extensive network of neurites projecting into the developing mucosa, with many Tuj1+ neurites present at the basolateral surface of the epithelial cell layer (Fig. 2*A*, Supplemental Movie S1: http://doi.org/10.5281/zenodo.3518046). At E16.5, neurites were present throughout the developing circular muscle and submucous cell layers, and the majority of villi also contained Tuj1-immunoreactive neurites (Fig. 2*B*, Supplemental Movie S2: http://doi.org/10.5281/zenodo.3518194. Very few Tuj1+ cell bodies were detected in the submucous plexus at either E14.5 or E16.5 (Fig. 2).

Neurochemistry of neurites innervating the lamina propria. We first used immunohistochemistry against neuronal nitric oxide synthase (nNOS) to identify the neurochemistry of the fibers, as nNOS-immunoreactive neurites were previously described in villi at E18.5 (57). nNOS+ fibers appeared in the gut in a time-dependent manner. Our results show that nNOS+ fibers were not present at E14.5 ($n = 0/6$, data not shown), and only a very few were detected in two out of six E16.5 preparations ($n = 2/6$, data not shown). nNOS+ fibers were clearly present in the gut by P0 ($n = 6/6$ gut samples, Fig. 3*A*). The cholinergic markers ChAT and vAChT did not label any fibers at any of the embryonic ages (data not shown). To exclude the possibility of bias resulting from low sensitivity of the antisera in the gastrointestinal tract, we also used *ChAT-Cre;R26R-YFP* mice as a genetic tool to investigate the timing of mucosal innervation by cholinergic neurons. Faint YFP+ fibers were observed at P0 ($n = 3/4$, Fig. 3*B*), but not at E14.5 ($n = 0/4$) or E16.5 ($n = 0/5$). We tested two other markers (neurofilament-M and calcitonin gene-related peptide, CGRP) that are characteristically expressed by IPANs in the adult mouse (43). We detected neurofilament-M-immunoreactive neurites extending toward the mucosa at E14.5 (Fig. 3*C*), E16.5, and P0. However, although neurofilament-M is specific for IPANs in the adult mouse (43), subtype specificity is not guaranteed during development, as Young et al. (58) reported
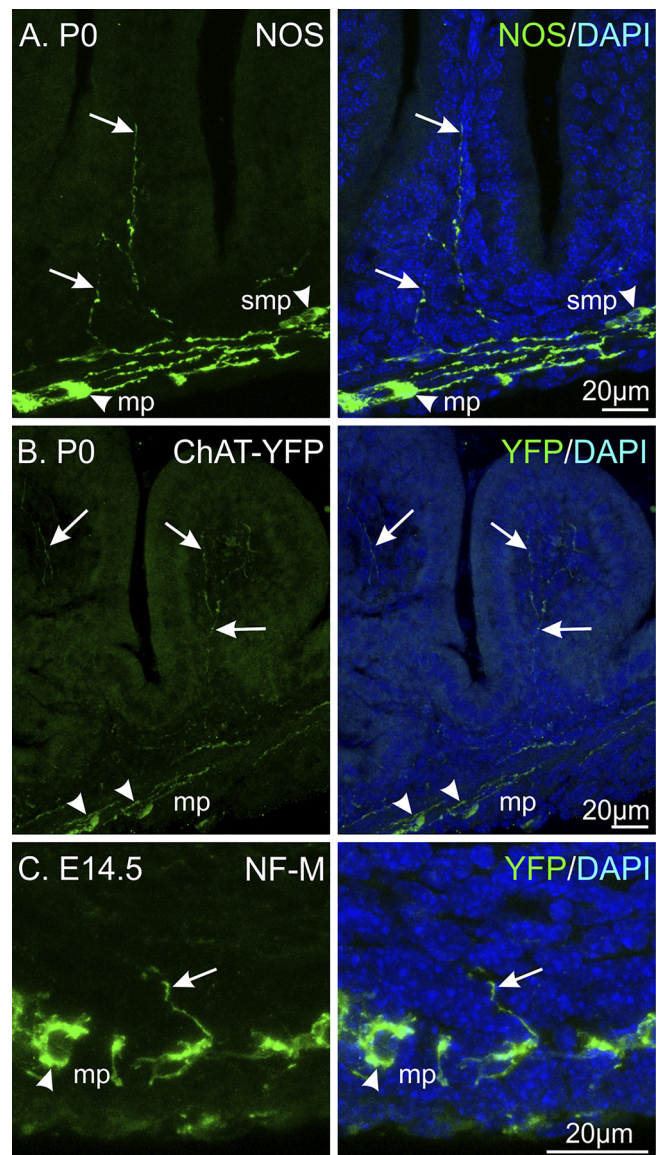

Fig. 3. Neurochemical phenotype of projections in the mucosa. *A*: many villi were observed to contain neuronal nitric oxide synthase (nNOS)-immunoreactive fibers at P0 (arrows), with cell bodies in both the myenteric (mp) and submucous plexus (smp; arrowheads). *B*: cholinergic fibers were examined using *ChAT-cre;R26R-YFP* mice, very few faint yellow fluorescent protein (YFP)+ fibers were observed in the mucosa at P0 (arrows), and cell bodies can be identified in the outer plexus layer (arrowheads). *C*: neurofilament-M (NF-M) immunoreactive fibers were observed in the mucosa at E14.5 (arrows). Cell bodies were present in the myenteric plexus (arrowheads).

neurofilament-M expression in all enteric neurons at E11.5. Unlike neurofilament-M, CGRP-immunoreactive neurites were not detected in the mucosa between E14.5 and E16.5 (data not shown), which is in line with previous work by Branchek and Gershon (9), who reported that CGRP immunoreactivity in the cell bodies of myenteric neurons is first detected at E17.5.

First projections to the mucosa arise from the myenteric plexus. In the mature ENS, both myenteric and submucous neurons project to the gut mucosa (18). During development, the submucous plexus arises from a secondary migration of enteric neural crest-derived cells (ENCCs) from the myenteric plexus (28, 49). We found that the appearance of neurites

in the lamina propria, which was first observed at E13.5, preceded the formation of submucous ganglia. ENCCs were observed in the submucous plexus region from E15.5 onward in *Wnt1-Cre;R26R-GCaMP3* mice, but only 14.5% of GFP+ cells in the presumptive submucous plexus expressed the pan-neuronal marker Hu (117 cells from six E15.5 and E16.5 gut preparations, Fig. 4*A*). Consistent with these data, 83.5% of GFP+ submucous plexus ENCCs were immunoreactive for Sox10 (Fig. 4; 85 cells from 5 E15.5 and E16.5 gut preparations, Fig. 4*B*), which is expressed by neural precursors and glial cells but not neurons (56). In the myenteric plexus at the same age, $56.9 \pm 1.7\%$ of GFP+ cells were identified to be Hu+, while $31.3 \pm 1.2\%$ were Sox10+ (299 cells from 4 E15.5-E16.5 gut preparations). The proportions of Sox10+ and neuronal cells are consistent with a previous study (56) and show that neuronal differentiation in the myenteric plexus is more advanced than in the submucous plexus. Therefore, it appears that the first enteric neurons to innervate the lamina propria at E13.5 are myenteric neurons, but it is likely that submucosal neurons also contribute to the mucosal innervation after E15.5.

Enteric neurites in the mucosa transmit electrical signals as early as E15.5. To examine the ability of neurites in the mucosa to conduct electrical signals, live calcium imaging was performed using intact preparations of rostral small intestine from *Wnt1-Cre;R26R-GCaMP3* mice at various ages. A focal stimulating electrode was placed on the tip of an individual villus (Fig. 5, *A* and *A'*), or in the case of E14.5 preparations, on the surface of the mucosa, where the generated electrical field activates the neurites in the vicinity. In adult small intestine, electrical stimulation triggered intracellular Ca^{2+} ($[Ca^{2+}]_i$) responses in subpopulations of enteric neurons in both the myenteric and submucous plexuses (Fig. 5, *B–C*"; Table 2; Supplemental Movie S3: https://doi.org/10.5281/zenodo.3518231). Electrical stimulation of individual villus tips also triggered $[Ca^{2+}]_i$ transients in the myenteric plexus at P0 (*n* = 19/20, Table 2, Fig. 5, *D–D*"), E16.5 (*n* = 12/12, Fig. 5, *E–E*"), and E15.5 (*n* = 14/19, Fig. 5, *F–F*", Supplemental Movie S4: https://doi.org/10.5281/zenodo.3518231). The fact that distinct responder cells are surrounded by unresponsive ones (Fig. 5) and do not appear in a concentric pattern, confirms that specific projections are present and excludes the possibility that the electric field activates neuronal cell bodies in the plexus layers directly. Very few cells were responsive at E15.5, making up only 3.5% of the total number of cells visible in the field of view (Table 2). This proportion of responsive cells in each field of view increases with age, but this may be dependent on changes in enteric network density that occur with time (Table 2, Fig. 5). At E14.5, stimulation of the mucosa surface also triggered $[Ca^{2+}]_i$ transients in myenteric neurons (Fig. 5, *G–G*"). However, at this age, it is possible that some cell bodies were directly stimulated, as the mucosa is very thin at E14.5 and villi have not yet formed.

The amplitude of the Ca^{2+} transients increased from E15.5 to P0, but decreased between P0 and adult (Fig. 5*H*). In the embryonic gut, the responses were abolished by the application of the voltage-dependent Na^+ channel inhibitor, tetrodotoxin (TTX; 1 μM; only 2/33 cells continued to respond to electrical stimulation in TTX and their $[Ca^{2+}]_i$ amplitudes were reduced; Fig. 5*I*). The timing of responses varied within each preparation. For example, in the adult submucous plexus and at E15.5, the peaks of the $[Ca^{2+}]_i$ transients do not occur simultaneously (Fig. 5, *C*" and *F*"). However, it is currently difficult to draw conclusions about response timing, as the kinetics of the GCaMP proteins are not necessarily fast enough to discriminate events at this timescale (7). This is further complicated by contractions of the gut muscle (Supplemental Movie S4, https://doi.org/10.5281/zenodo.3518231), which appear to be mediated by myogenic activity that is at embryonic ages insensitive to inhibition of L-type voltage-dependent Ca^{2+} channels by nifedipine (45).

To examine the contribution of fast cholinergic transmission, we applied the nicotinic receptor antagonist hexamethonium to preparations of P0 small intestine (*n* = 3). Because a supramaximal concentration (200 μM) of hexamethonium did not reduce the number of responding neurons, we conclude that fast nicotinic transmission is not involved in this signaling pathway.
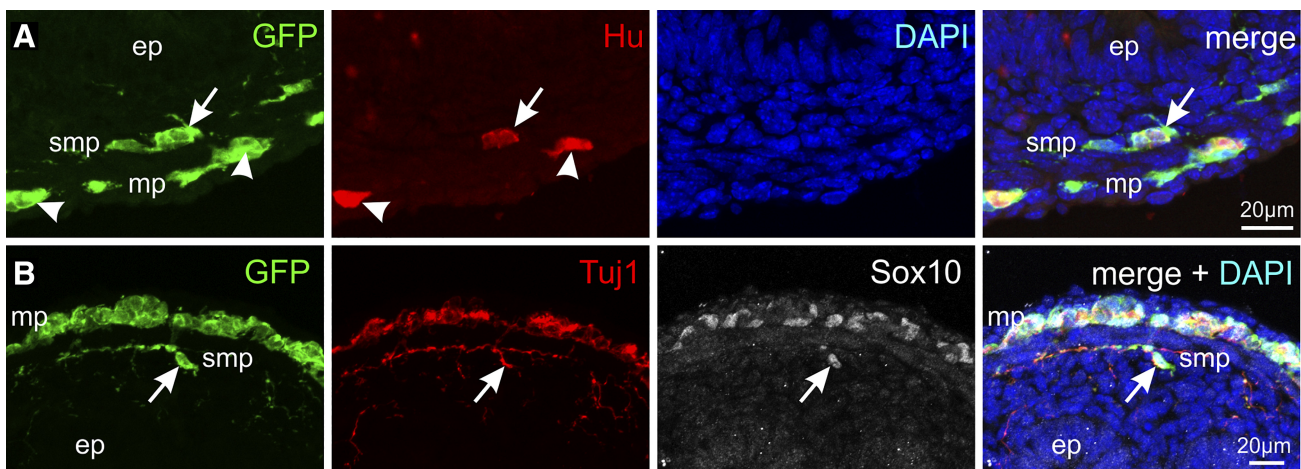

Fig. 4. Confocal images of transverse cryosections of E16.5 *Wnt1-CRE;R26R-GCaMP3* gut. The submucous plexus can be seen as green fluorescent protein-positive (GFP+) cells that are distinct from the more densely populated myenteric plexus. *A*: some GFP+ submucous cells are also Hu+ (arrows). Although more Hu+ cell bodies are present in the myenteric plexus (arrowheads). *B*: majority of GFP+ submucous cells are Sox10+ (arrows). Tuj1 neurites are present in the submucous plexus (arrow), but cell bodies are sparse; there is only one GFP+ cell in the submucous plexus in this cryosection and it is Sox10+.

Postnatal enteric neurons respond to 5-HT stimulation of neurite terminals. We also investigated the ability of enteric neurons to respond to 5-HT applied directly to their neurite terminals within the mucosa. 5-HT (10 μM) was applied into villi using a micropipette coupled to a pressurized picospritzer, while the pipette was pushed through the epithelial surface of the villus (Fig. 6A). Thus, 5-HT could be injected into the villus to directly act on nerve terminals in the mucosa, mimicking the release of 5-HT from the basolateral surface of enterochromaffin cells. To ensure $[Ca^{2+}]_i$ transients were not elicited by activation of mechanosensitive elements due to pressurized spritz injections, controls were performed where Krebs solution was injected into villus tips. The injection of control Krebs solution did not produce detectable activation of $[Ca^{2+}]_i$ transients in enteric neurons (Fig. 6, *B–B"*; Table 2). The volume of solution injected was calculated to be 5.5 ± 0.8 nl ($n = 3$).

In the adult small intestine, 5-HT injections elicited $[Ca^{2+}]_i$ transients in myenteric neurons in the majority of adult preparations (Fig. 6, *C–C"*; Table 2; Supplemental Movie S5, https://doi.org/10.5281/zenodo.3518231). Responses to 5-HT were blocked by the 5-HT$_3$R antagonist, ondansetron (Fig. 6*D*; 0/48 cells from $n = 9$ gut preparations), while the cholinergic nicotinic blocker hexamethonium did not reduce the number of responders ($n = 8$ adult gut preparations).

Post hoc immunohistochemistry was performed to examine the morphology and neurochemistry of neurons responding to 5-HT injections. 5-HT-responsive myenteric neurons had larger cell diameters compared with Hu+ nonresponsive neurons (Fig. 6, *E–E"'*). As described above, neurofilament-M and CGRP are distinct markers of IPANs in the adult mouse (43). Therefore, we examined whether 5-HT-responsive neurons were immunoreactive for these markers. None of the neurons responsive to 5-HT injections were immunoreactive for neurofilament-M, and we found very few neurofilament-M+ cells in any preparations examined (data not shown). In addition, we were unable to obtain successful staining of CGRP in cell bodies to identify whether 5-HT responsive cells were CGRP-immunoreactive. IPANs also express calbindin, although in the mouse not all calbindin+ cells are IPANs (43). We found that 71 ± 13% of 5-HT responsive neurons were immunoreactive for calbindin (Fig. 6, *F–F"'*, 29 cells from seven gut preparations). Both "strong" and "faint" immunoreactivity to calbindin has previously been reported in the mouse (43), and both
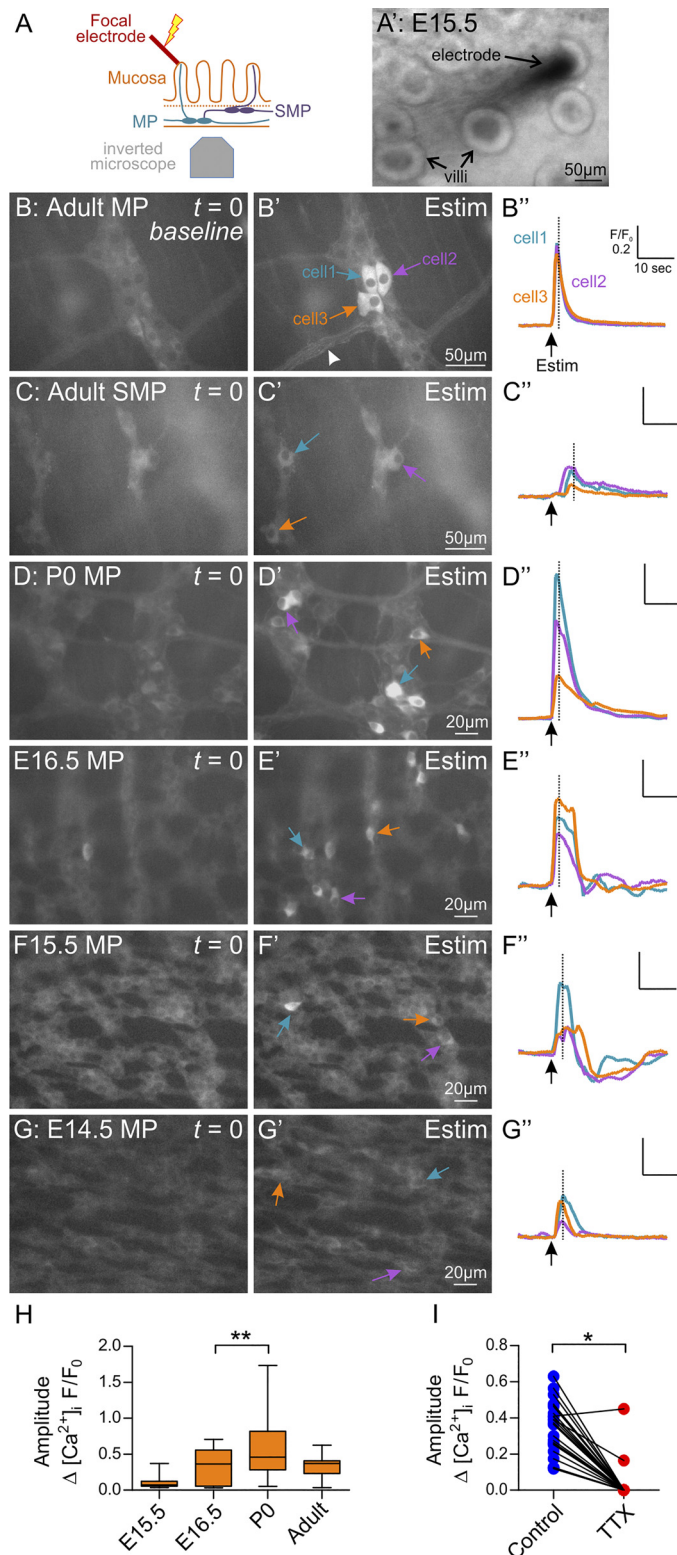

Fig. 5. Responses of enteric neurons to focal electrical stimulation at the villus tip in the small intestine. *A*: diagram of gut preparation and imaging setup. The small intestine was kept intact as much as possible to preserve all cell layers. The focal electrode was placed on a villus tip, and calcium imaging was performed simultaneously on myenteric or submucosal neurons. *A'*: transmitted light image of the electrode positioning on an embryonic preparation. *B–G"*: representative images of $[Ca^{2+}]_i$ transients in the adult myenteric plexus (MP; *B–B"*), adult submucous plexus (SMP; *C–C"*), and the myenteric plexus of P0 (P0 MP; *D–D"*), embryonic day 16.5 (E16.5; *E–E"*), embryonic day E15.5 (E15.5; *F–F"*), and embryonic day (E14.5; *G–G"*) gut. Cells responsive to electrical stimulation of villi are highlighted by arrows: blue arrows denote *cell 1*, purple arrows denote *cell 2*, and orange arrows denote *cell 3*. Traces from individually labeled cells are shown *B"*, *C"*, *D"*, *E"*, *F"*, and *G"*), all drawn to the same scale. Time point of images shown in *B'*, *C'*, *D'*, *E'*, *F'*, and *G'* are indicated by a dotted line in *B"*, *C"*, *D"*, *E"*, *F"*, and *G"*, where the arrowhead shows the time of the electrical stimulation (Estim). *H*: box and whisker plot of the amplitude of $[Ca^{2+}]_i$ transients in cells responsive to electrical stimulation at E15.5, E16.5, P0, and adult (numbers of responding cells examined at each age are: 50 cells at E15.5, 45 cells at E16.5, 83 cells at P0, 10 cells at the adult stage; **$P < 0.01$; one-way ANOVA with Bonferroni post hoc test). Box shows means ± SD, whiskers the entire range of data. *I*: amplitude of responses in control conditions and after application of TTX at E16.5. TTX abolished responses in the majority of cells and significantly decreased response amplitude (*$P < 0.0001$, paired *t* test, $n = 28$ cells).

Table 2. *Responses to various villi stimuli*

	Average Total Number of Cells per Field of View*	Electrical Stimulation	5-HT Injection into Villus	Krebs Injection Into Villus	5-HT onto Epithelium Surface	Krebs onto Epithelium Surface
Adult	31 ± 2	$6.5 \pm 2\%$ ($n = 4/8$**)	$25.2 \pm 3\%$ ($n = 29/35$)	($n = 0/14$)	$11.2 \pm 4\%$ ($n = 12/40$)	4.5% ($n = 1/20$)
P7	72 ± 5	na	$18.3 \pm 3\%$ ($n = 13/14$)	($n = 0/4$)	$11.7 \pm 4\%$ ($n = 5/12$)	($n = 0/4$)
P0	122 ± 8	$13.2 \pm 2\%$ ($n = 19/20$)	$8.6 \pm 2\%$ ($n = 12/21$)	na	$1 \pm 0.3\%$ ($n = 2/12$)	na
E16.5	147 ± 19	$10.7 \pm 5\%$ ($n = 12/12$)	($n = 0/4$)	($n = 0/4$)	($n = 0/4$)	na
E15.5	214 ± 42	$3.5 \pm 1\%$ ($n = 14/19$)	na	na	na	na

Values are expressed as means $\pm$ SE of the percentage of cells responding to each stimulation; n = number of responsive gut preparations/total gut preparations examined. E, embryonic day; na, not applicable; P, postnatal day; 5-HT, serotonin. *Please note: there are large differences in the total number of cells visible per field of view between the different ages, as enteric neural crest-derived cells are more densely packed in the younger gut and individual ganglia are less distinct. **In adult electrical stimulation, although sometimes responsive cell bodies were not observed, responsive fibers were present in 7/8 preparations.

populations were found to respond to 5-HT (Fig. 6, *F–F"*). Approximately half of 5-HT responsive cells were also immunoreactive for calretinin ($42 \pm 12\%$, Fig. 6, *G –G'''*, 25 cells from 7 gut preparations), but none were nNOS+ (data not shown, 54 cells from 14 preparations).

To examine the development of responses to 5-HT, recordings were also performed in E16.5, P0, and P7 mice. At P7, 5-HT injections triggered $[Ca^{2+}]_i$ transients in many cells and responses appeared similar to adult preparations (Fig. 7, *A–A"*; Supplemental Movie S6, https://doi.org/10.5281/zenodo.3518231). At P0, $[Ca^{2+}]_i$ transients in response to 5-HT injections were observed in ~50% of preparations examined (Fig. 7, *B–B"*; Table 2). The total number of responding cells and the amplitude of responses were difficult to calculate at P0 due to spontaneous contractions and also spontaneous $[Ca^{2+}]_i$ transients. Of the preparations that remained stable during recording, the amplitude of responses was significantly smaller at P0 compared with P7 and adult (Fig. 7*C*). No responses were observed to 5-HT at E16.5 ($n = 4$, data not shown); however, as the villi were quite small and short, it was not possible to determine whether we had successfully placed the micropipette into the mucosa beneath the epithelial surface.

Responses to 5-HT on the gut epithelial surface. In addition to basolateral release, 5-HT is also released into the gut lumen (5, 55), and previous studies have shown that 5-HT application to the epithelial surface evokes action potentials in enteric neurons (6, 24). We therefore also applied 5-HT onto the epithelial surface using a micropipette and picospritzer (Fig. 8*A*). Although many GCaMP3-expressing cells were visible in each field of view, detectable $[Ca^{2+}]_i$ transients were only observed in 30% of adult preparations examined (Table 2; Fig. 8, *B–B"*). The amplitude of responses was smaller than when 5-HT was injected into the villus (0.19 ± 0.02 F/F$_0$, $n = 35$ cells vs 0.45 ± 0.02 F/F$_0$, $n = 186$ cells; $P < 0.0001$, Student's t-test). The differences in the appearance of $[Ca^{2+}]_i$ transients between responses elicited by 5-HT spritzed onto the epithelial surface versus 5-HT injected into the villi are most likely due to different mechanisms of enteric neuron activation. 5-HT spritzed onto the epithelial surface will activate enteroendocrine cells that may then communicate with enteric neurites via release of various compounds, possibly including 5-HT itself. Whereas, 5-HT injected into the mucosa acts directly on nerve terminals.

Responses to epithelial surface application of 5-HT were also examined at E16.5, P0 and P7. No cells responded at

E16.5, however, small responses would have been difficult to detect because there was also spontaneous activity. At P0, only two cells were observed to respond to application of 5-HT to the gut epithelium out of 12 gut preparations examined (Table 2). By P7, there was an increase in both the proportion of responsive preparations (Table 2) and the amplitude of $[Ca^{2+}]_i$ responses (Fig. 8, *C–D*).

DISCUSSION

The detection of luminal contents by enteric neurons is a crucial first step in the control of motility induced by ingested food and in the regulation of gut function by the microbiota. In this study, we examined the anatomical and functional development of the innervation of the mucosa. We show that neurites extend from the myenteric plexus, forming close associations with the basolateral surface of the intestinal epithelium by E14.5, and transmit electrical signals by E15.5. Responses to 5-HT applied to the terminals of mucosal projecting neurons were recorded at birth.

The first neurites innervating the mucosa come from the myenteric plexus. Previously, immunohistochemical studies have reported innervation of the mouse intestinal mucosa at E16 (10) and E18.5 (57). Recently, one study in the developing chick gut has also revealed neurites projecting to the mucosa at E16.5 (13). Our study shows that the first neurites to innervate the mucosa are present as early as E13.5, preceding the formation of the submucous plexus. Therefore, the first cells to innervate the mucosa appear to come from the myenteric plexus. Some of the mucosal innervation may also arise from extrinsic neurons, as vagal fibers are present in the proximal small intestine by E16.5 (44). However, extrinsic innervation is unlikely to account for the high density of fibers present in the mucosa at embryonic ages. Additionally, focal electrical stimulation of villus tips resulted in $[Ca^{2+}]_i$ transients in cell bodies in the myenteric plexus at E15.5.

After the formation of submucous ganglia, it was not possible to identify the relative contribution of projections from the myenteric versus submucous ganglia at different ages. The extension of neurites to the mucosa occurs at a similar time to the migration of ENCCs from the myenteric to submucous plexus, which involves the GDNF/Ret/GFRα1 and DCC/netrin signaling pathways (28, 49). It is possible that similar signals attract neurites to extend out of the myenteric plexus centripetally toward the mucosa. Hedgehog signaling has been proposed to inhibit the
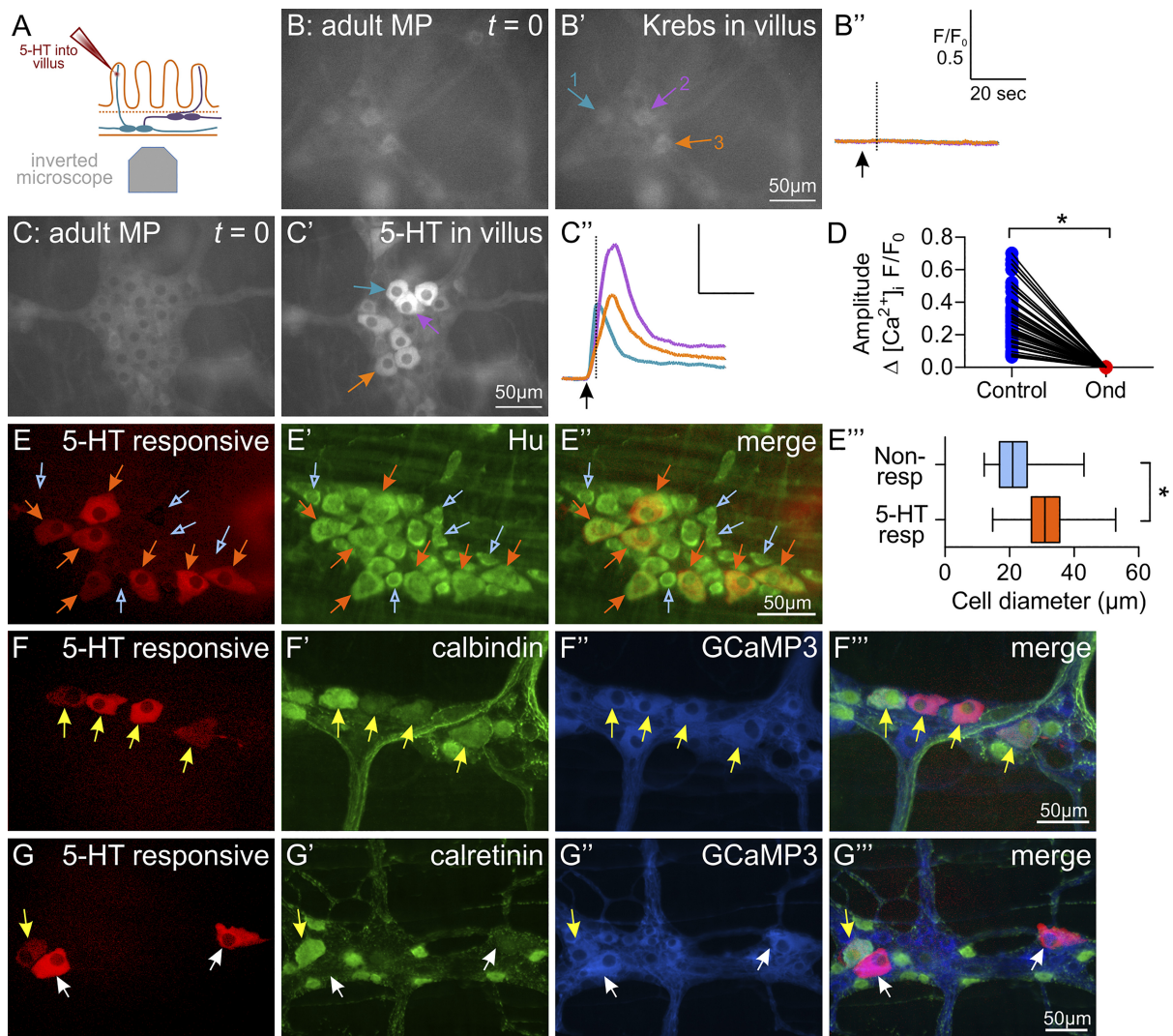
Fig. 6. Responses of adult myenteric neurons to 5-HT injected into mucosa. *A*: diagram of gut preparation and positioning of spritz pipette beneath epithelial surface for application of 5-HT directly onto neurite terminals. *B–B"*: representative responses of control Krebs solution injected into villus. Traces from three cells are shown (blue arrows denote *cell 1*, purple arrows denote *cell 2*, and orange arrows denote *cell 3*), and no change in $[Ca^{2+}]_i$ could be detected after injection of Krebs. *C–C"*: representative responses to 5-HT injection into the mucosa in adult myenteric neurons. Time point of images shown in *B'* and *C'* are indicated by a dotted line in *B"* and *C"*. *D*: changes in $[Ca^{2+}]_i$ responses to 5-HT injections in control Krebs and after application of ondansetron (Ond). Ondansetron abolished all responses to 5-HT (*$P < 0.0001$; paired *t*-test; $n = 48$). *E–E"*: identification of diameters of cells responding to 5-HT injections and nonresponsive cells using post hoc Hu immunolabelling. 5-HT-responsive cells (orange arrows; *E*) were identified after post hoc immunohistochemistry for Hu (*E'*). The diameters of nonresponsive Hu+ cells, some of which are shown by blue open arrows, in the same fields of view were also measured. The merged images are shown in *E"*. *E'''*: Box and whisker plot of the diameters of 5-HT responsive and nonresponsive neurons. 5-HT-responsive neurons ($n = 55$) had significantly larger diameters compared with nonresponsive neurons ($n = 177$; *$P < 0.0001$; Student's *t* test). *F* and *G'''*: post hoc identification of 5-HT-responsive cells using immunohistochemistry against calbindin (*F–F'''*) and calretinin (*G–G'''*). The amplitude of calcium responses is shown by the intensity of the fluorescence in *F* and *G*. 5-HT-responsive cells that are also calbindin+ or calretinin+ are indicated by yellow arrows. Other 5-HT-responsive cells that are not immunoreactive for these markers are indicated by white arrows.

projection of neurites toward the mucosa during embryonic development (29); however, in their study, neurites were not observed at E18.5 in wild-type mice, and earlier ages were not examined. The discrepancy between this study and our data could be due to differences in the region of the gut examined. In our study, the rostral half of the small intestine was investigated in all experiments; it is unclear which region of small intestine was examined by Jin et al. (29).

Development of IPANs and electrical circuits. There is evidence for postnatal development of IPANs, as cells exhibiting AH-electrophysiology and Dogiel type II morphology have been detected at P0 (17), but not at E11.5 and E12.5 (25).

Furthermore, myenteric IPANs express CGRP in the adult mouse, which has not been detected before E17.5 (9). In the current study, it was not possible to determine the neurochemical coding of the myenteric neurons projecting to the mucosa during prenatal development. They are most likely to be IPANs, which would suggest that these neurons develop earlier than previously reported, and this could have important implications on the development of enteric neural circuitry. However, we cannot rule out the possibility that embryonic mucosal neurites arise from enteric neurons that project there transiently, particularly as some neurites express nNOS, which is not found in adult mucosal fibers (57).
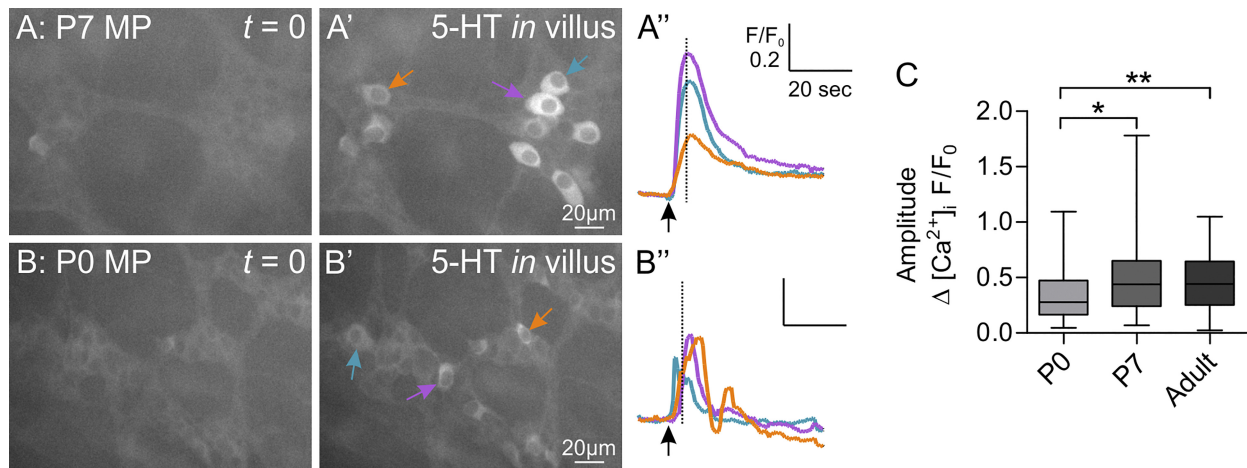
Fig. 7. Responses of postnatal myenteric neurons to 5-HT injected into mucosa. *A–B"*: representative responses to 5-HT injection of myenteric neurons at postnatal *day 7* (P7) (*A–A"*) and P0 (*B–B"*). Time-point of images shown in *A'* and *B'* are indicated by a dotted line in *A"* and *B"*. *C*: amplitudes of $[Ca^{2+}]_i$ transients in cells responsive to 5-HT injections. $[Ca^{2+}]_i$ responses are significantly smaller at P0 compared with P7 and adult (*$P < 0.01$, **$P < 0.001$; one-way ANOVA with Bonferroni post hoc test; numbers of cells responding at each age are 64 cells at P0, 155 cells at P7, and 86 cells in adult gut). Blue arrows denote *cell 1*, purple arrows denote *cell 2*, and orange arrows denote *cell 3*.

As early as E15.5, stimulation of villi tips by focal electrical stimulation triggered $[Ca^{2+}]_i$ responses in cell bodies in the myenteric plexus. These responses were blocked by TTX, indicating that action potentials were elicited and were needed to generate detectable $[Ca^{2+}]_i$ responses. Although excitatory nicotinic neurotransmission is present in the ENS as early as E14.5 (16), application of hexamethonium did not reduce the responses to electrical stimulation in our study, suggesting that nicotinic transmission was not involved.

Responses to 5-HT by adult neurons. The gut epithelium is the largest source of 5-HT in the body (22). It has been assumed that 5-HT released from enterochromaffin cells directly communicates with enteric neurons. Our study is the first to show that enteric neurons respond to 5-HT applied to the gut mucosa, beneath the epithelium. Although this mimics 5-HT release from enterochromaffin cells, further investigation will be necessary to also prove that endogenous 5-HT released from

these cells activates mucosal processes of enteric neurons. The downstream effects of enteric neuron activation require further investigation. Although 5-HT from the gut mucosa can regulate and modulate colonic motility (2, 26), intestinal transit time is not affected in Tph1-knockout mice, which lack mucosal 5-HT (37). For a comprehensive review on the role of 5-HT in the control of colonic motility, we refer to Keating and Spencer (33). Whether 5-HT released from the enterochromaffin cells influences other aspects of gut function, such as secretion or communication with the CNS, needs to be examined.

On the basis of their neurochemical coding and cell body size, myenteric neurons responding to 5-HT injected into the mucosa are likely to be IPANs. Responses to 5-HT appear to be mediated by $5-HT_3$ receptors, as all responses were abolished in the presence of ondansetron. Post hoc immunohistochemistry showed that ~30% of 5-HT-responsive cells were
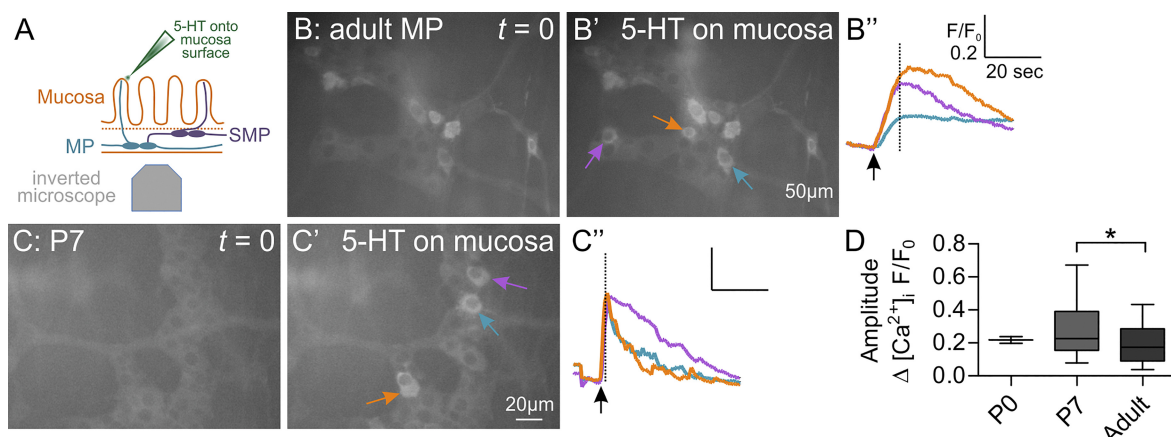

Fig. 8. Responses of enteric neurons to 5-HT application onto epithelial surface. *A*: diagram of gut preparation and pressurized 5-HT spritz onto gut epithelium. *B–C"*: representative images of responses in adult (*B–B"*) and P7 (*C–C"*) myenteric neurons to 5-HT spritz. Responding cells are highlighted by arrows (blue arrows denote *cell 1*, purple arrows denote *cell 2*, and orange arrows denote *cell 3*) and representative traces from individual cells shown (*B"* and *C"*). Time point of images shown in *B'* and *C'* are indicated by a dotted line in *B"* and *C"*. *D*: box and whisker plot of amplitudes to 5-HT spritz onto epithelial surface at P0, P7, and adult (*$P < 0.05$; one-way ANOVA with Bonferroni post hoc test; numbers of cells found to respond to 5-HT spritz at each age are: 2 cells at P0, 31 cells at P7, and 35 cells in the adult gut). MP, myenteric plexus; P7, postnatal *day 7*; SMP, submucous plexus; 5-HT, serotonin.

not immunoreactive for calbindin, suggesting that they were not IPANs. Using the current GCaMP-based technology, it was not possible to determine conclusively which neurons were directly activated by 5-HT application and which ones were indirectly activated via synaptic communication. Our hexamethonium data suggest that at least fast nicotinic transmission is not involved. The responsive fields of IPANs in the mucosa have been mapped previously using dye tracing and electrophysiological recordings in the adult guinea pig ileum, where cell bodies tend to closely underlie the villi they functionally innervate (4, 46). This is in line with findings by Lasrado et al. (36), who described that clonal units organize themselves in a columnar fashion to form the functional ENS.

So far, intrinsic sensory neurons with the electrophysiological, morphological, and neurochemical characteristics of IPANs have not been identified in the submucous plexus of the mouse (40, 52). Our functional Ca^{2+} imaging data show that a population of adult submucous neurons responds to 5-HT. However, whether these are IPANs or secretomotor neurons remains to be investigated, as all submucous neurons, at least in humans, appear to express the 5-HT$_3$ receptor (39). It is also possible that these submucosal neurons are synaptically activated by myenteric neurons.

We also investigated the ability of enteric neurons to respond to 5-HT release into the gut lumen and onto the epithelial surface. Previously, 5-HT applied to mucosa surfaces was found to elicit action potentials in enteric neurons (6, 24). Although we did detect some responses to 5-HT applied to the epithelial surface, in most cases, only a few cells responded with a small $[Ca^{2+}]_i$ transient. As several action potentials are needed to elicit a visible $[Ca^{2+}]_i$ transient, it is possible that smaller responses were not detected using GCaMP3 (54).

Maturation of the gut epithelium and the development of neuronal responses to mucosal 5-HT. During development, the appearance of different epithelial cell types has been identified as early as E18.5 (11, 21). While the appearance of different enteroendocrine cells has not been extensively examined, immunoreactivity to 5-HT in the gut epithelium has been shown at E16.5 (9). Our results show that by birth, neurons were responsive to 5-HT applied directly to neurite terminals in the small intestine villi. It is possible that this response is present before birth, as 5-HT$_3$R mRNA has been detected in the gut at E14.5 (48); however, this was technically difficult to examine. There is significant maturation of 5-HT responses in the first postnatal week, which may reflect maturation of the mucosa, as well as changes in the ENS as the gut becomes responsible for nutrient absorption. Changes may also arise due to colonization of the gut by the microbiota, which has been shown to influence postnatal ENS development, including enteric glial migration (14, 27, 30, 42). Additionally, the presence of microbiota can enhance 5-HT release from enteroendocrine cells into the gut lumen (55).

Conclusions. Overall, our data show that the gastrointestinal mucosa is innervated by myenteric neurons before the formation of intestinal villi. Neurites conduct electrical signals and respond to exogenous 5-HT applied to their terminals by birth. The communication between enteroendocrine cells and nerve terminals appears to develop later. This early innervation of the gut mucosa could have important implications on the development of intrinsic sensory neurons and the formation of neural circuits in the ENS.

DISCLOSURES

No conflicts of interest, financial or otherwise, are declared by the authors.

AUTHOR CONTRIBUTIONS

M.M.H., W.B., and P.V.B. conceived and designed research; M.M.H., C.F., and K.L. performed experiments; M.M.H., C.F., and K.L. analyzed data; M.M.H., C.F., W.B., and P.V.B. interpreted results of experiments; M.M.H. prepared figures; M.M.H. drafted manuscript; M.M.H., C.F., W.B., J.T., and P.V.B. edited and revised manuscript; W.B., J.T., and P.V.B. approved final version of manuscript.

REFERENCES

1. **Alcaino C, Knutson KR, Treichel AJ, Yildiz G, Strege PR, Linden DR, Li JH, Leiter AB, Szurszewski JH, Farrugia G, Beyder A.** A population of gut epithelial enterochromaffin cells is mechanosensitive and requires Piezo2 to convert force into serotonin release. *Proc Natl Acad Sci USA* 115: E7632–E7641, 2018. doi:10.1073/pnas.1804938115.
2. **Balasuriya GK, Hill-Yardin EL, Gershon MD, Bornstein JC.** A sexually dimorphic effect of cholera toxin: rapid changes in colonic motility mediated via a 5-HT3 receptor-dependent pathway in female C57Bl/6 mice. *J Physiol* 594: 4325–4338, 2016. doi:10.1113/JP272071.
3. **Bellono NW, Bayrer JR, Leitch DB, Castro J, Zhang C, O'Donnell TA, Brierley SM, Ingraham HA, Julius D.** Enterochromaffin cells are gut chemosensors that couple to sensory neural pathways. *Cell* 170: 185–198.e16, 2017. doi:10.1016/j.cell.2017.05.034.
4. **Bertrand PP, Kunze WA, Bornstein JC, Furness JB.** Electrical mapping of the projections of intrinsic primary afferent neurones to the mucosa of the guinea-pig small intestine. *Neurogastroenterol Motil* 10: 533–542, 1998. doi:10.1046/j.1365-2982.1998.00128.x.
5. **Bertrand PP.** Real-time measurement of serotonin release and motility in guinea pig ileum. *J Physiol* 577: 689–704, 2006. doi:10.1113/jphysiol.2006.117804.
6. **Bertrand PP, Kunze WAA, Furness JB, Bornstein JC.** The terminals of myenteric intrinsic primary afferent neurons of the guinea-pig ileum are excited by 5-hydroxytryptamine acting at 5-hydroxytryptamine-3 receptors. *Neuroscience* 101: 459–469, 2000. doi:10.1016/S0306-4522(00)00363-8.
7. **Boesmans W, Hao MM, Vanden Berghe P.** Optogenetic and chemogenetic techniques for neurogastroenterology. *Nat Rev Gastroenterol Hepatol* 15: 21–38, 2018. doi:10.1038/nrgastro.2017.151.
8. **Boesmans W, Martens MA, Weltens N, Hao MM, Tack J, Cirillo C, Vanden Berghe P.** Imaging neuron-glia interactions in the enteric nervous system. *Front Cell Neurosci* 7: 183, 2013. doi:10.3389/fncel.2013.00183.
9. **Branchek TA, Gershon MD.** Time course of expression of neuropeptide Y, calcitonin gene-related peptide, and NADPH diaphorase activity in neurons of the developing murine bowel and the appearance of 5-hydroxytryptamine in mucosal enterochromaffin cells. *J Comp Neurol* 285: 262–273, 1989. doi:10.1002/cne.902850208.
10. **Breau MA, Pietri T, Eder O, Blanche M, Brakebusch C, Fässler R, Thiery JP, Dufour S.** Lack of β1 integrins in enteric neural crest cells leads to a Hirschsprung-like phenotype. *Development* 133: 1725–1734, 2006. doi:10.1242/dev.02346.
11. **Bry L, Falk P, Huttner K, Ouellette A, Midtvedt T, Gordon JI.** Paneth cell differentiation in the developing intestine of normal and transgenic

mice. *Proc Natl Acad Sci USA* 91: 10335–10339, 1994. doi:10.1073/pnas.91.22.10335.

12. **Bülbring E, Crema A.** The release of 5-hydroxytryptamine in relation to pressure exerted on the intestinal mucosa. *J Physiol* 146: 18–28, 1959. doi:10.1113/jphysiol.1959.sp006175.

13. **Chevalier NR, Dacher N, Jacques C, Langlois L, Guedj C, Faklaris O.** Embryogenesis of the peristaltic reflex. *J Physiol* 597: 2785–2801, 2019. doi:10.1113/JP277746.

14. **Collins J, Borojevic R, Verdu EF, Huizinga JD, Ratcliffe EM.** Intestinal microbiota influence the early postnatal development of the enteric nervous system. *Neurogastroenterol Motil* 26: 98–107, 2014. doi:10.1111/nmo.12236.

15. **Danielian PS, Muccino D, Rowitch DH, Michael SK, McMahon AP.** Modification of gene activity in mouse embryos in utero by a tamoxifen-inducible form of Cre recombinase. *Curr Biol* 8: 1323–1326, 1998. doi:10.1016/S0960-9822(07)00562-3.

16. **Foong JPP, Hirst CS, Hao MM, McKeown SJ, Boesmans W, Young HM, Bornstein JC, Vanden Berghe P.** Changes in nicotinic neurotransmission during enteric nervous system development. *J Neurosci* 35: 7106–7115, 2015. doi:10.1523/JNEUROSCI.4175-14.2015.

17. **Foong JPP, Nguyen TV, Furness JB, Bornstein JC, Young HM.** Myenteric neurons of the mouse small intestine undergo significant electrophysiological and morphological changes during postnatal development. *J Physiol* 590: 2375–2390, 2012. doi:10.1113/jphysiol.2011.225938.

18. **Furness JB.** Types of neurons in the enteric nervous system. *J Auton Nerv Syst* 81: 87–96, 2000. doi:10.1016/S0165-1838(00)00127-2.

19. **Furness JB, Kunze WAA, Bertrand PP, Clerc N, Bornstein JC.** Intrinsic primary afferent neurons of the intestine. *Prog Neurobiol* 54: 1–18, 1998. doi:10.1016/S0301-0082(97)00051-8.

20. **Furness JB, Rivera LR, Cho HJ, Bravo DM, Callaghan B.** The gut as a sensory organ. *Nat Rev Gastroenterol Hepatol* 10: 729–740, 2013. doi:10.1038/nrgastro.2013.180.

21. **Garcia MI, Ghiani M, Lefort A, Libert F, Strollo S, Vassart G.** LGR5 deficiency deregulates Wnt signaling and leads to precocious Paneth cell differentiation in the fetal intestine. *Dev Biol* 331: 58–67, 2009. doi:10.1016/j.ydbio.2009.04.020.

22. **Gershon MD, Tack J.** The serotonin signaling system: from basic understanding to drug development for functional GI disorders. *Gastroenterology* 132: 397–414, 2007. doi:10.1053/j.gastro.2006.11.002.

23. **Gribble FM, Reimann F.** Signalling in the gut endocrine axis. *Physiol Behav* 176: 183–188, 2017. doi:10.1016/j.physbeh.2017.02.039.

24. **Gwynne RM, Bornstein JC.** Local inhibitory reflexes excited by mucosal application of nutrient amino acids in guinea pig jejunum. *Am J Physiol Gastrointest Liver Physiol* 292: G1660–G1670, 2007. doi:10.1152/ajpgi.00580.2006.

25. **Hao MM, Lomax AE, McKeown SJ, Reid CA, Young HM, Bornstein JC.** Early development of electrical excitability in the mouse enteric nervous system. *J Neurosci* 32: 10949–10960, 2012. doi:10.1523/JNEUROSCI.1426-12.2012.

26. **Heredia DJ, Gershon MD, Koh SD, Corrigan RD, Okamoto T, Smith TK.** Important role of mucosal serotonin in colonic propulsion and peristaltic reflexes: in vitro analyses in mice lacking tryptophan hydroxylase 1. *J Physiol* 591: 5939–5957, 2013. doi:10.1113/jphysiol.2013.256230.

27. **Hung LY, Boonma P, Unterweger P, Parathan P, Haag A, Luna RA, Bornstein JC, Savidge TC, Foong JPP.** Neonatal antibiotics disrupt motility and enteric neural circuits in mouse colon. *Cell Mol Gastroenterol Hepatol* 8: 298–300.e6, 2019. doi:10.1016/j.jcmgh.2019.04.009.

28. **Jiang Y, Liu MT, Gershon MD.** Netrins and DCC in the guidance of migrating neral crest-derived cells in the developing bowel and pancreas. *Dev Biol* 258: 364–384, 2003. doi:10.1016/S0012-1606(03)00136-2.

29. **Jin S, Martinelli DC, Zheng X, Tessier-Lavigne M, Fan C-M.** Gas1 is a receptor for sonic hedgehog to repel enteric axons. *Proc Natl Acad Sci USA* 112: E73–E80, 2015. doi:10.1073/pnas.1418629112.

30. **Kabouridis PS, Lasrado R, McCallum S, Chng SH, Snippert HJ, Clevers H, Pettersson S, Pachnis V.** Microbiota controls the homeostasis of glial cells in the gut lamina propria. *Neuron* 85: 289–295, 2015. doi:10.1016/j.neuron.2014.12.037.

31. **Kaelberer MM, Buchanan KL, Klein ME, Barth BB, Montoya MM, Shen X, Bohórquez DV.** A gut-brain neural circuit for nutrient sensory transduction. *Science* 361: eaat5236, 2018. doi:10.1126/science.aat5236.

32. **Keating DJ, Spencer NJ.** Release of 5-hydroxytryptamine from the mucosa is not required for the generation or propagation of colonic migrating motor complexes. *Gastroenterology* 138: 659–670.e2, 2010. doi:10.1053/j.gastro.2009.09.020.

33. **Keating DJ, Spencer NJ.** What is the role of endogenous gut serotonin in the control of gastrointestinal motility? *Pharmacol Res* 140: 50–55, 2019. doi:10.1016/j.phrs.2018.06.017.

34. **Kirchgessner AL, Tamir H, Gershon MD.** Identification and stimulation by serotonin of intrinsic sensory neurons of the submucosal plexus of the guinea pig gut: activity-induced expression of Fos immunoreactivity. *J Neurosci* 12: 235–248, 1992. doi:10.1523/JNEUROSCI.12-01-00235.1992.

35. **Kunze WAA, Bornstein JC, Furness JB.** Identification of sensory nerve cells in a peripheral organ (the intestine) of a mammal. *Neuroscience* 66: 1–4, 1995. doi:10.1016/0306-4522(95)00067-S.

36. **Lasrado R, Boesmans W, Kleinjung J, Pin C, Bell D, Bhaw L, McCallum S, Zong H, Luo L, Clevers H, Vanden Berghe P, Pachnis V.** Lineage-dependent spatial and functional organization of the mammalian enteric nervous system. *Science* 356: 722–726, 2017. doi:10.1126/science.aam7511.

37. **Li Z, Chalazonitis A, Huang YY, Mann JJ, Margolis KG, Yang QM, Kim DO, Côté F, Mallet J, Gershon MD.** Essential roles of enteric neuronal serotonin in gastrointestinal motility and the development/survival of enteric dopaminergic neurons. *J Neurosci* 31: 8998–9009, 2011. doi:10.1523/JNEUROSCI.6684-10.2011.

38. **Martin AM, Lumsden AL, Young RL, Jessup CF, Spencer NJ, Keating DJ.** The nutrient-sensing repertoires of mouse enterochromaffin cells differ between duodenum and colon. *Neurogastroenterol Motil* 29: e13046, 2017. doi:10.1111/nmo.13046.

39. **Michel K, Zeller F, Langer R, Nekarda H, Kruger D, Dover TJ, Brady CA, Barnes NM, Schemann M.** Serotonin excites neurons in the human submucous plexus via 5-HT3 receptors. *Gastroenterology* 128: 1317–1326, 2005. doi:10.1053/j.gastro.2005.02.005.

40. **Mongardi Fantaguzzi C, Thacker M, Chiocchetti R, Furness JB.** Identification of neuron types in the submucosal ganglia of the mouse ileum. *Cell Tissue Res* 336: 179–189, 2009. doi:10.1007/s00441-009-0773-2.

41. **Noah TK, Donahue B, Shroyer NF.** Intestinal development and differentiation. *Exp Cell Res* 317: 2702–2710, 2011. doi:10.1016/j.yexcr.2011.09.006.

42. **Obata Y, Pachnis V.** The effect of microbiota and the immune system on the development and organization of the enteric nervous system. *Gastroenterology* 151: 836–844, 2016. doi:10.1053/j.gastro.2016.07.044.

43. **Qu ZD, Thacker M, Castelucci P, Bagyánszki M, Epstein ML, Furness JB.** Immunohistochemical analysis of neuron types in the mouse small intestine. *Cell Tissue Res* 334: 147–161, 2008. doi:10.1007/s00441-008-0684-7.

44. **Ratcliffe EM, Fan L, Mohammed TJ, Anderson M, Chalazonitis A, Gershon MD.** Enteric neurons synthesize netrins and are essential for the development of the vagal sensory innervation of the fetal gut. *Dev Neurobiol* 71: 362–373, 2011. doi:10.1002/dneu.20869.

45. **Roberts RR, Ellis M, Gwynne RM, Bergner AJ, Lewis MD, Beckett EA, Bornstein JC, Young HM.** The first intestinal motility patterns in fetal mice are not mediated by neurons or interstitial cells of Cajal. *J Physiol* 588: 1153–1169, 2010. doi:10.1113/jphysiol.2009.185421.

46. **Song ZM, Brookes SJH, Costa M.** Identification of myenteric neurons which project to the mucosa of the guinea-pig small intestine. *Neurosci Lett* 129: 294–298, 1991. doi:10.1016/0304-3940(91)90484-B.

47. **Spencer NJ, Nicholas SJ, Robinson L, Kyloh M, Flack N, Brookes SJ, Zagorodnyuk VP, Keating DJ.** Mechanisms underlying distension-evoked peristalsis in guinea pig distal colon: is there a role for enterochromaffin cells? *Am J Physiol Gastrointest Liver Physiol* 301: G519–G527, 2011. doi:10.1152/ajpgi.00101.2011.

48. **Tecott L, Shtrom S, Julius D.** Expression of a serotonin-gated ion channel in embryonic neural and nonneural tissues. *Mol Cell Neurosci* 6: 43–55, 1995. doi:10.1006/mcne.1995.1005.

49. **Uesaka T, Nagashimada M, Enomoto H.** GDNF signaling levels control migration and neuronal differentiation of enteric ganglion precursors. *J Neurosci* 33: 16372–16382, 2013. doi:10.1523/JNEUROSCI.2079-13.2013.

50. **Vanden Berghe P, Kenyon JL, Smith TK.** Mitochondrial Ca^{2+} uptake regulates the excitability of myenteric neurons. *J Neurosci* 22: 6962–6971, 2002. doi:10.1523/JNEUROSCI.22-16-06962.2002.

51. **Vincent AD, Wang XY, Parsons SP, Khan WI, Huizinga JD.** Abnormal absorptive colonic motor activity in germ-free mice is rectified by butyrate, an effect possibly mediated by mucosal serotonin. *Am J Physiol Gastrointest Liver Physiol* 315: G896–G907, 2018. doi:10.1152/ajpgi.00237.2017.

52. **Wong V, Blennerhassett M, Vanner S.** Electrophysiological and morphological properties of submucosal neurons in the mouse distal colon.

Neurogastroenterol Motil 20: 725–734, 2008. doi:10.1111/j.1365-2982. 2008.01117.x.

53. **Yadav VK, Balaji S, Suresh PS, Liu XS, Lu X, Li Z, Guo XE, Mann JJ, Balapure AK, Gershon MD, Medhamurthy R, Vidal M, Karsenty G, Ducy P.** Pharmacological inhibition of gut-derived serotonin synthesis is a potential bone anabolic treatment for osteoporosis. *Nat Med* 16: 308–312, 2010. doi:10.1038/nm.2098.

54. **Yamada Y, Mikoshiba K.** Quantitative comparison of novel GCaMP-type genetically encoded Ca^{2+} indicators in mammalian neurons. *Front Cell Neurosci* 6: 41, 2012. doi:10.3389/fncel.2012.00041.

55. **Yano JM, Yu K, Donaldson GP, Shastri GG, Ann P, Ma L, Nagler CR, Ismagilov RF, Mazmanian SK, Hsiao EY.** Indigenous bacteria from the gut microbiota regulate host serotonin biosynthesis. *Cell* 161: 264– 276, 2015. doi:10.1016/j.cell.2015.02.047.

56. **Young HM, Bergner AJ, Müller T.** Acquisition of neuronal and glial markers by neural crest-derived cells in the mouse intestine. *J Comp Neurol* 456: 1–11, 2003. doi:10.1002/cne.10448.

57. **Young HM, Ciampoli D.** Transient expression of neuronal nitric oxide synthase by neurons of the submucous plexus of the mouse small intestine. *Cell Tissue Res* 291: 395–401, 1998. doi:10.1007/s004410051009.

58. **Young HM, Jones BR, McKeown SJ.** The projections of early enteric neurons are influenced by the direction of neural crest cell migration. *J Neurosci* 22: 6005–6018, 2002. doi:10.1523/JNEUROSCI.22-14-06005.2002.

59. **Zagorodnyuk VP, Spencer NJ.** Localization of the sensory neurons and mechanoreceptors required for stretch-evoked colonic migrating motor complexes in mouse colon. *Front Physiol* 2: 98, 2011. doi:10.3389/fphys.2011.00098.

60. **Zariwala HA, Borghuis BG, Hoogland TM, Madisen L, Tian L, De Zeeuw CI, Zeng H, Looger LL, Svoboda K, Chen TW.** A Cre-dependent GCaMP3 reporter mouse for neuronal imaging *in vivo*. *J Neurosci* 32: 3131–3141, 2012. doi:10.1523/JNEUROSCI.4469-11.2012.